Optical pumping of rubidium atoms frozen in solid argon

Andrew N. Kanagin, Sameer K. Regmi, Pawan Pathak, and Jonathan D. Weinstein*
Department of Physics, University of Nevada, Reno, Nevada 89557, USA
(Received 27 September 2013; published 6 December 2013)

We have grown crystals of solid argon doped with rubidium atoms. The spectrum of the implanted atoms depends on the crystal-growth temperature and annealing history. We have used optical pumping to polarize the spin state of the implanted atoms and polarization spectroscopy to detect the spin state and measure the spin-relaxation time. In addition to the desired optical pumping, we also observed modification of the absorption spectrum of the rubidium due to the applied light.

DOI: 10.1103/PhysRevA.88.063404 PACS number(s): 32.80.Xx, 32.30.−r, 07.55.Ge

I. INTRODUCTION

Matrix isolation spectroscopy, in which molecules of interest are implanted in crystals of inert gases, is a powerful technique for studying reactive molecules at high densities [1]. It is also of interest in atomic physics: crystals can be grown with very high densities of dopant atoms; the implanted species may be held in the same location indefinitely; and because of their relatively weak interaction with the host matrix, implanted atoms retain many of the properties of free atoms [2]. This technique has potential applications in tests of the standard model in atomic [3] and molecular [4] systems. It has potential applications in quantum information, either using individual atoms as qubits or using large numbers of atoms in high-optical-depth samples for ensemble-based quantum information protocols. In addition, it is a promising system for atomic magnetometry.

Gas-phase alkali-metal magnetometers are currently the most sensitive detectors of magnetic fields [5,6]. The standard quantum limit for the magnetic field sensitivity, assuming the atomic spin state can be prepared and detected with high efficiency, is $B = \sqrt{2/nVT_2t\gamma^2}$, where t is the measurement time, γ is the atom's gyromagnetic ratio, T_2 is the spin coherence time, V is the volume of the atomic sample, and n is its density [7]. For two atomic samples of the same volume and γ, their relative sensitivity will be determined by nT_2. The coherence time of high-field atomic magnetometers is limited by spin-exchange collisions, which limits the figure of merit to $nT_2 \approx 1 \times 10^9$ cm^{-3} s [7]. The spin-exchange relaxation-free (SERF) magnetometer is not limited by spin-exchange collisions; for atomic potassium, spin-relaxation collisions limit the figure of merit to $nT_2 \approx 2 \times 10^{13}$ cm^{-3} s [8,9]. However, SERF magnetometers can operate only at low fields and have not yet reached their fundamental sensitivity limit.

Prior work examining the electron spin resonance spectra of rubidium atoms frozen in a solid argon matrix provides a lower limit on the coherence time of $T_2 \geqslant 4 \times 10^{-8}$ s at a rubidium density of $n \approx 1 \times 10^{19}$ cm^{-3} [10,11]. Even with this minimum value for T_2, the matrix isolation system would have a figure of merit of $nT_2 \approx 4 \times 10^{11}$ cm^{-3} s, higher than non-SERF atomic vapor magnetometers. We note that this figure of merit is comparable to state of the art for nitrogen-vacancy magnetometers [12,13]. Much like nitrogen-vacancy magnetometers, because the matrix isolated atoms do not move, the technique can be extended to small-size scales at which vapor-cell magnetometry is impractical. However, none of this can be achieved unless one can prepare and detect the spin state of the implanted atoms with high efficiency.

Weis and collaborators have shown that it is possible to optically pump alkali-metal atoms in solid helium [14,15]. Cesium in solid helium has a T_1 time of $\sim$1 s [14] and T_2 times $\geqslant 0.1$ s [16]; the nature of the relaxation is not yet understood [17]. While helium would make a seemingly ideal host matrix, it has considerable technical difficulties due to the fact that it only forms a solid at high pressure. Consequently, the crystal cannot be grown by the usual method of vapor deposition. Instead, a pure helium crystal is formed in a pressure cell and is subsequently doped, typically by laser ablation. To date, dopant densities have been limited to $\sim 10^9$ cm^{-3} [17]. This is significantly lower than the densities possible in other cryogenic noble gas matrices, such as argon, neon [18], and molecular hydrogen [19].

In prior work, the optical spectroscopy of rubidium atoms in an argon matrix was investigated. It was found that if a small atomic polarization was induced by applying a large magnetic field, that polarization could be detected optically [10]. Herein, we explore the optical manipulation of the spin of rubidium atoms in an argon host matrix using diode lasers.

II. CRYSTAL GROWTH AND ANNEALING

The rubidium-doped argon crystals were grown on a 5-mm-thick sapphire substrate, mounted to a vertical copper plate which was cooled by a pulse tube cooler [20]. A small oven containing a 99.75% pure rubidium sample was positioned roughly 5 cm away, with its 0.5-mm-diameter nozzle aimed at the sapphire plate. The oven and sapphire plate each had resistive heaters, and their temperatures were monitored by a platinum resistor and a calibrated diode, respectively.

Crystals were grown by flowing argon through the oven. By adjusting the argon pressure and the oven temperature, the fluxes of argon and rubidium could be controlled. The argon gas used was 99.998% pure. Cooling the argon fill line to dry ice temperatures (to reduce impurities) made no discernible difference in the crystals formed.

Crystal thickness was monitored during deposition using thin-film interferometry. Typically, crystals were grown at a rate of 1 μm/min to thicknesses on the order of 100 μm [21]. The crystal thickness was not uniform and varied roughly

*weinstein@physics.unr.edu; http://www.physics.unr.edu/xap/

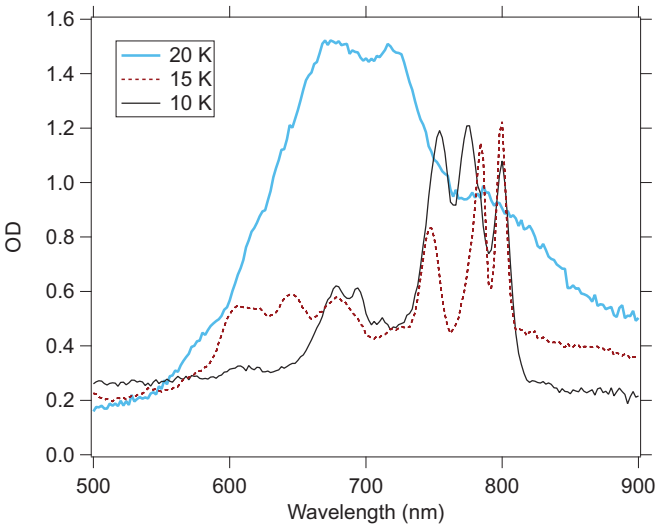

FIG. 1. (Color online) Spectra of rubidium-doped argon crystals grown at different substrate temperatures. The transmission of the crystal $T = e^{-\mathrm{OD}}$. All spectra were taken at 3.2 K.

linearly across the crystal face. The thicknesses at the ends of the crystal differed from the central thickness by roughly $\pm 40\%$.

Traditionally, matrix isolation experiments grow argon crystals at temperatures $\gtrsim$20 K to enable the crystal to anneal [1]. We have grown crystals with sapphire substrate temperatures ranging from 3.2 to 20 K. After growing the crystal, the substrate was cooled to the cryostat's base temperature of 3.2 K.

We performed absorption spectroscopy using a halogen light source and a grating spectrometer. Typical spectra are shown in Fig. 1. Crystals grown at 20 K are spectrally broad, with no resolved peaks. Crystals grown at a substrate temperature of 15 K show a triplet of peaks at 800, 783, and 747 nm, with additional spectral features at shorter wavelengths. Crystals grown at 10 K similarly show three resolved peaks but at wavelengths which are consistently shifted from the 15 K values, with peaks at 800, 777, and 753 nm. The 10 K spectrum also shows a second triplet of partially resolved peaks at 712, 696, and 679 nm.

The wavelengths of the spectral lines of the crystal grown at 10 K are consistent with those previously measured by Kupferman and Pipkin for crystals grown at 4 K [10]. In that work, all lines are attributed to the $5s \rightarrow 5p$ transition of rubidium. Each triplet arises from the splitting of the $5p$ level of rubidium due to the crystal-field potential. The fact that there are two triplets is attributed to two different trapping sites.

We attribute the off-resonance scattering of light to the crystal itself, which has hundreds of cracks. At growth temperatures below 10 K, the light scattering by the crystal increases. Crystals grown at 7 K have the same line positions as the 10 K crystal but have higher OD's off resonance. For crystals grown at 3.2 K substrate temperatures, the OD from argon alone is so high that we did not investigate doping the crystals with rubidium.

We calculate the density of rubidium in the crystal from the absorption spectrum and our thickness measurements. Typical densities are on the order of 10^{17} cm^{-3} [22].

After growing and cooling the crystals, we investigated annealing the crystals by heating them, holding at an elevated temperature for roughly 10^2 s, and cooling back to the base temperature. After annealing, the rubidium spectrum typically changes to the spectrum of a crystal grown at the annealing temperature. This change is irreversible, and typically, the off-resonance OD increases with every annealing cycle.

III. BLEACHING

Once a crystal had been grown and its spectra measured with white-light spectroscopy, we attempted to optically pump the spin states of the implanted rubidium atoms using narrow-band laser light. This revealed an unexpected and unfortunate phenomenon: the applied light caused a modification of the crystal's absorption spectrum. We call this effect "bleaching," which can be seen in the data in Fig. 2.

Applying light at 800 nm causes a decrease in absorption at 800 nm and affects other regions of the spectrum as well. In crystals grown at 15 K, all three peaks of the triplet of lines around 775 nm decrease in absorption. In crystals grown at 10 K, we observe a splitting of the 800-nm peak into two features, but there is little change in the OD of the other two peaks of the triplet. For both types of crystal, the bleaching is accompanied by an increase in the absorption at 700 nm. If, instead, we apply a laser on resonance with the middle peak of the triplet (783 nm for the crystal grown at 15 K and 777 nm for the crystal grown at 10 K), both crystals exhibit behavior similar to their response to the 800-nm laser.

As discussed above, the triplet around 775 nm was attributed to one type of trapping site, while the absorption

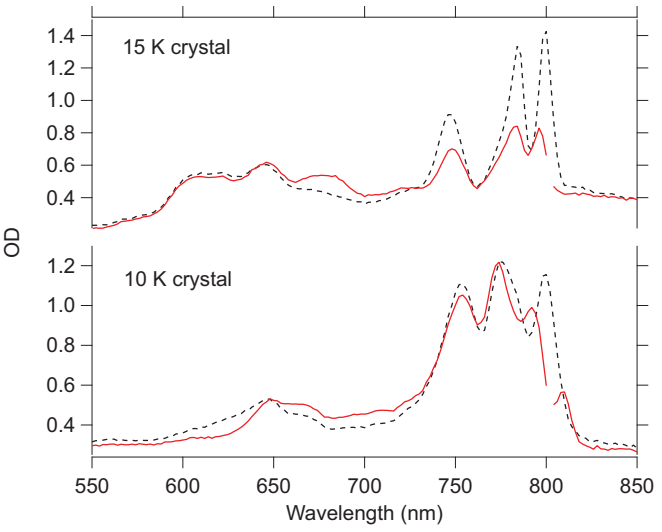

FIG. 2. (Color online) Spectra illustrating bleaching of the crystal by the laser for a crystal grown at 15 K (upper trace) and a crystal grown at 10 K (lower trace). All spectra were taken at a 3.2 K substrate temperature. The dashed lines are spectra taken with the crystal exposed to the halogen light source. The solid lines are spectra taken with both the halogen light source and an 802-nm laser with an intensity of 3 mW/cm^2.

around 700 nm is attributed to a second trapping site [10]. The observed changes in the spectrum indicate that the light is causing the atoms to be transferred from one type of trapping site to the other. From measuring the bleaching as a function of time and from our density measurements, we calculate that an atom will scatter roughly 10^1 photons before bleaching. The bleaching spectra also reveal the nature of the broadening: crystals grown at 15 K exhibit almost entirely homogeneous broadening, while crystals grown at 10 K exhibit a mix of homogeneous and inhomogeneous broadening.

If a bleached crystal is left in the dark, its spectrum will remain bleached for a time longer than 15 hours. However, if light is applied, the bleaching can be reversed. White light applied to the crystal will restore the original spectrum. Similarly, light from a 690-nm light-emitting diode (LED; 20-nm FWHM) will restore the absorption at 800 nm. Bleaching by the 800-nm laser was always observed to be reversible. However, the 690-nm light caused an irreversible change in the spectrum, which can be seen by comparing the spectra of the 10 K crystal in Figs. 1 and 2. After applying the 690-nm light, the three partially resolved peaks near 700 nm disappear and do not return with time or with subsequent application of white light or 800-nm light.

IV. OPTICAL PUMPING OF SPIN

We monitor the polarization of the spin state of the rubidium atoms with a weak probe beam. Typical probe beam intensities are 100 μW/cm^2 at a wavelength of 802 nm. We chose to initially work at this wavelength because the 800-nm peak showed the greatest sensitivity to atomic polarization in prior work [10]. The incident probe beam is linearly polarized, and the transmitted beam is split into its right-hand circularly polarized (RHC) and left-hand circularly polarized (LHC) components, which are monitored on two photodiodes.

To optically pump the atoms, a circularly polarized pump beam is briefly applied to the crystal. The pump beam wavelength is identical to the probe; typical pump intensities are on the order of 20 mW/cm^2. The pump causes bleaching and induces a polarization, as can be seen in Fig. 3. Because of the bleaching effects, light from our "debleaching" LED is applied continuously during these experiments.

An induced atomic polarization would cause LHC and RHC light to have different absorptions. This effect can be clearly seen in the upper traces of Fig. 3. However, we must verify that any such change is due to the atoms and not measurement error resulting from the combination of bleaching and the birefringence of the sapphire substrate. To verify this, we compare the optical pumping signal with a longitudinal magnetic field applied to the same signal with a transverse applied field; fields are 2 and 5 G, respectively. In the case of a longitudinal field, the atoms will be pumped into a stationary state and a large polarization will accumulate; in the case of a transverse field we expect negligible polarization. The data in Fig. 3 confirm that the differential change in absorption is due to the atomic polarization.

Once the atoms are polarized, the induced polarization decays with time. To extract the T1 time, we analyze the data as shown in Fig. 4. We calculate the ratio of the normalized photodetector voltages and take the difference between the data for longitudinal and transverse fields. The polarization typically shows exponential-like decay with time; however, it typically is not fit well by a single exponential. The data in Fig. 4 are fit to double exponential decay. The shorter exponential time constant is 70 ms. This time constant varies between the different crystals we have grown and is typically in the range of 50 to 100 ms.

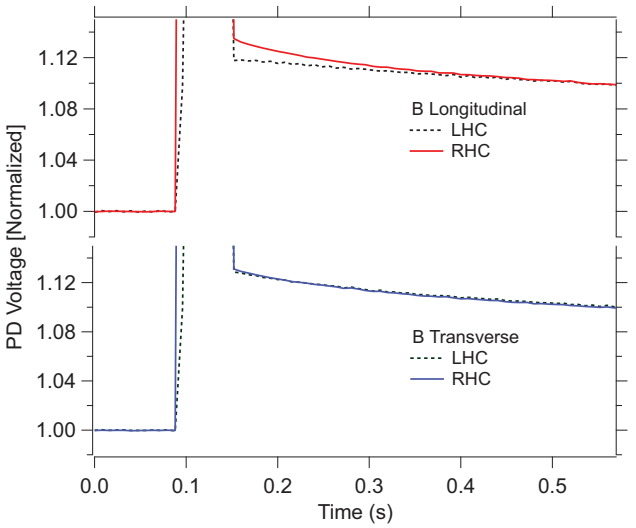

FIG. 3. (Color online) Optical pumping of rubidium atoms in an argon matrix grown at 10 K; the data are taken at a temperature of 3.2 K. The probe beam is on continuously; the RHC pumping beam is applied from 0.1 to 0.15 ms. The photodiode signals are shown for both the LHC and RHC detectors; the signals are normalized so that the level is 1 prior to optical pumping. The top graph is with a longitudinal magnetic field applied, and the bottom graph is with a transverse field applied.

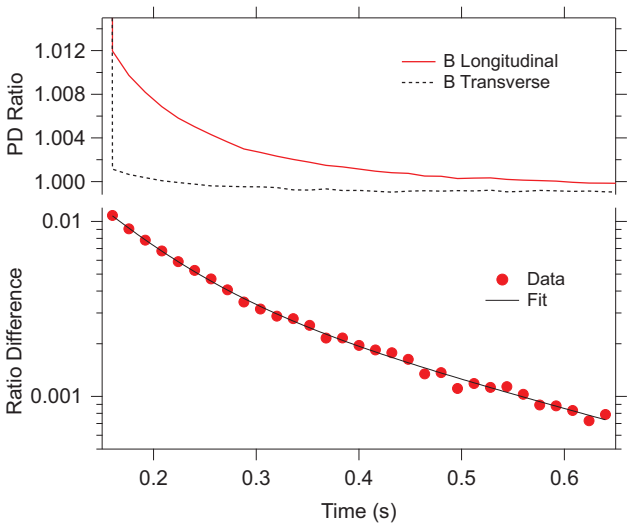

FIG. 4. (Color online) The upper graph shows the ratio of the LHC and RHC photodiode signals for longitudinal and transverse magnetic fields; the data are the same as presented in Fig. 3. The lower graph shows the difference between the two upper signals, fit as discussed in the text.

V. CONCLUSION AND DISCUSSION

We have demonstrated optical pumping of the spin state of rubidium atoms implanted in an argon matrix. The measured polarizations are small: the difference in the OD for LHC and RHC light is on the order of 10^{-2}, with an average OD of 1. If we optically pump and probe at 775 nm to address the central peak of the triplet of a crystal grown at 10 K, the observed polarization is typically four times smaller. This is consistent with prior measurements [10].

We attribute the small optical signal to the mixing of the fine-structure levels of the $5p$ excited state by the interaction with the argon crystal [10]. This mixing reduces the sensitivity of the absorption of different polarizations of light to the spin state of the ground-state atom, as does the unresolved hyperfine structure of rubidium. The small polarization signal and the bleaching effects are both disadvantageous for experiments using matrix-isolated atoms for magnetometry or quantum information experiments.

In future experiments, it would be of interest to explore other atom-matrix combinations. Recent experiments working with ytterbium atoms in solid neon did not exhibit the bleaching effects seen here [2]. Moreover, by choosing an atom with similar electronic structure but larger excited-state fine structure, along with a more weakly interacting lattice, one might find a regime where the fine-structure splitting is large compared to the interaction with the crystal. This would make optical detection of the spin state more sensitive. Some appealing dopant atoms are cesium and gold, with fine-structure splittings of 554 and 3816 cm^{-1}, considerably larger than rubidium's 238 cm^{-1} [22]. Matrices such as neon and parahydrogen may offer weaker interactions than argon while still allowing for doping at high densities [1,19].

ACKNOWLEDGMENTS

It is our pleasure to thank Wade J. Cline, Carl D. Davison, Jr., and Chase B. Hartzell for their assistance in the construction of the apparatus and Chase B. Hartzell for his assistance in growing crystals. We gratefully acknowledge helpful conversations with David Patterson and Robert S. Sheridan. This paper is based upon work supported by the National Science Foundation under Grants No. PHY 0903847 and No. PHY 1265905.

[1] S. Cradock and A. J. Hinchcliffe, *Matrix Isolation* (Cambridge University Press, Cambridge, 1975).
[2] C.-Y. Xu, S.-M. Hu, J. Singh, K. Bailey, Z.-T. Lu, P. Mueller, T. P. O'Connor, and U. Welp, Phys. Rev. Lett. **107**, 093001 (2011).
[3] M. Arndt, S. Kanorsky, A. Weis, and T. Hänsch, Phys. Lett. A **174**, 298 (1993).
[4] M. G. Kozlov and A. Derevianko, Phys. Rev. Lett. **97**, 063001 (2006).
[5] D. Budker and M. Romalis, Nat. Phys. **3**, 227 (2007).
[6] D. Budker and D. Kimball, *Optical Magnetometry* (Cambridge University Press, Cambridge, 2013).
[7] D. Sheng, S. Li, N. Dural, and M. V. Romalis, Phys. Rev. Lett. **110**, 160802 (2013).
[8] I. K. Kominis, T. W. Kornack, J. C. Allred, and M. V. Romalis, Nature (London) **422**, 596 (2003).
[9] T. W. Kornack, S. J. Smullin, S.-K. Lee, and M. V. Romalis, Appl. Phys. Lett. **90**, 223501 (2007).
[10] S. L. Kupferman and F. M. Pipkin, Phys. Rev. **166**, 207 (1968).
[11] R. H. Beaumont, H. Chihara, and J. A. Morrison, Proc. Phys. Soc. **78**, 1462 (1961).
[12] V. M. Acosta, E. Bauch, M. P. Ledbetter, C. Santori, K.-M. C. Fu, P. E. Barclay, R. G. Beausoleil, H. Linget, J. F. Roch, F. Treussart, S. Chemerisov, W. Gawlik, and D. Budker, Phys. Rev. B **80**, 115202 (2009).
[13] P. L. Stanwix, L. M. Pham, J. R. Maze, D. Le Sage, T. K. Yeung, P. Cappellaro, P. R. Hemmer, A. Yacoby, M. D. Lukin, and R. L. Walsworth, Phys. Rev. B **82**, 201201 (2010).
[14] M. Arndt, S. I. Kanorsky, A. Weis, and T. W. Hänsch, Phys. Rev. Lett. **74**, 1359 (1995).
[15] S. Lang, S. Kanorsky, T. Eichler, R. Müller-Siebert, T. W. Hänsch, and A. Weis, Phys. Rev. A **60**, 3867 (1999).
[16] S. I. Kanorsky, S. Lang, S. Lücke, S. B. Ross, T. W. Hänsch, and A. Weis, Phys. Rev. A **54**, R1010 (1996).
[17] P. Moroshkin, A. Hofer, S. Ulzega, and A. Weis, Fiz. Nizk. Temp (Kiev). **32**, 1297 (2006).
[18] T. Kanda and T. Ebisu, J. Phys. Soc. Jpn. **31**, 957 (1971).
[19] T. Momose and T. Shida, Bull. Chem. Soc. Jpn. **71**, 1 (1998).
[20] S. K. Regmi, Master's thesis, University of Nevada, Reno, 2013.
[21] A. C. Sinnock, J. Phys. C **13**, 2375 (1980).
[22] J. E. Sansonetti, W. C. Martin, and S. L. Young, *Handbook of Basic Atomic Spectroscopic Data* (National Institute of Standards and Technology, Gaithersburg, MD, 2006), http://physics.nist.gov/PhysRefData/Handbook/.